Energy Model of an Air Source Heat Pump to Explore Performance Improvements under Cold Conditions: A Python Framework

Preprint

Conrado Ermel,[1,2] Marcus V.A. Bianchi,[1] and Paulo S. Schneider[2]

1 National Renewable Energy Laboratory
2 Federal University of Rio Grande do Sul

Presented at the 7th International High Performance Buildings Conference
West Lafayette, Indiana
July 10-14, 2022

NREL is a national laboratory of the U.S. Department of Energy
Office of Energy Efficiency & Renewable Energy
Operated by the Alliance for Sustainable Energy, LLC

This report is available at no cost from the National Renewable Energy Laboratory (NREL) at www.nrel.gov/publications.

Contract No. DE-AC36-08GO28308

Conference Paper
NREL/CP-5500-82753
January 2023

Energy Model of an Air Source Heat Pump to Explore Performance Improvements under Cold Conditions: A Python Framework

Preprint

Conrado Ermel,[1,2] Marcus V.A. Bianchi,[1] and Paulo S. Schneider[2]

1 National Renewable Energy Laboratory
2 Federal University of Rio Grande do Sul

Suggested Citation
Ermel, Conrado, Marcus V.A. Bianchi, and Paulo S. Schneider. 2023. *Energy Model of an Air Source Heat Pump to Explore Performance Improvements under Cold Conditions: A Python Framework: Preprint*. Golden, CO: National Renewable Energy Laboratory. NREL/CP-5500-82753. https://www.nrel.gov/docs/fy23osti/82753.pdf.

NREL is a national laboratory of the U.S. Department of Energy
Office of Energy Efficiency & Renewable Energy
Operated by the Alliance for Sustainable Energy, LLC

This report is available at no cost from the National Renewable Energy Laboratory (NREL) at www.nrel.gov/publications.

Contract No. DE-AC36-08GO28308

Conference Paper
NREL/CP-5500-82753
January 2023

National Renewable Energy Laboratory
15013 Denver West Parkway
Golden, CO 80401
303-275-3000 • www.nrel.gov

NOTICE

This work was authored in part by the National Renewable Energy Laboratory, operated by Alliance for Sustainable Energy, LLC, for the U.S. Department of Energy (DOE) under Contract No. DE-AC36-08GO28308. Funding provided by the U.S. Department of Energy Office of Energy Efficiency and Renewable Energy Building Technologies Office. The views expressed herein do not necessarily represent the views of the DOE or the U.S. Government. The U.S. Government retains and the publisher, by accepting the article for publication, acknowledges that the U.S. Government retains a nonexclusive, paid-up, irrevocable, worldwide license to publish or reproduce the published form of this work, or allow others to do so, for U.S. Government purposes.

Cover Photos by Dennis Schroeder: (clockwise, left to right) NREL 51934, NREL 45897, NREL 42160, NREL 45891, NREL 48097, NREL 46526.

Energy Model of an Air Source Heat Pump to Explore Performance Improvements under Cold Conditions: a Python Framework

Conrado ERMEL[1,2*], Marcus V.A. BIANCHI[1], Paulo S.SCHNEIDER[2]

[1] National Renewable Energy Laboratory - NREL,
Golden, Colorado, USA
conradoermel@gmail.com; Marcus.Bianchi@nrel.gov

[2] Federal University of Rio Grande do Sul, Department of Mechanical Engineering,
Porto Alegre, Rio Grande do Sul, Brazil
pss@mecanica.ufrgs.br

* Corresponding Author

ABSTRACT

Replacing combustion appliances with heat pumps can be part of a strategy to electrify buildings. When their electricity is supplied by renewables, the adoption of heat pumps for space heating may help curb the CO_2 emissions inherent to traditional heating systems that burn natural gas or coal. When operating in very cold climates, however, heat pump performance deteriorates, sometimes requiring backup heating supplied by electric resistances or other sources to continue to function. To avoid the use of electric resistances, complementary technologies, like thermal energy storage, solar collectors, or alternative refrigerants, have been explored in recent years. In this study, we present an open-source Python-based numerical model developed to evaluate the annual hourly performance of an air source heat pump (ASHP) operating in the USA. Simulation results include coefficient of performance and heating capacity. The model, validated with experimental results, will be employed in the future to investigate the feasibility of integrating thermal energy storage and other technologies into ASHPs operating in cold climates.

1. INTRODUCTION

Heat pumps can support the transition from fossil fuel appliances to electrified heating systems, which may foster the decarbonization of the building sector (Le et al., 2019). Heat pumps can supply heating demands up to five times more efficiently than electric resistances by running a vapor compression cycle (Dincer et al., 2017). The higher efficiency aligned with the fast growth of renewables' share in the world energy mix suggest an increase in the deployment of heat pumps in the near future (Bianco et al., 2017). There have been several recent scientific publications exploring the adoption of heat pumps to replace combustion appliances. Most of those studies rely on simulation models, a less expensive option than experiments, and an increasing number of simulation platforms for heat pumps have been documented.

Heat pump models can be structured as unified solutions (one single expression correlating the performance with independent parameters). Unified solutions consist of using regressions and generic correlations with experimental data to obtain the heat pump coefficient of performance (COP). These black-box models lead to very simple expressions, which can be solved with low computational effort. However, because they are curve fittings for specific equipment, the results are limited because no extrapolation can be made (Lyden, 2020).

Alternatively one can create separate models for each component because it facilitates exchanging the components (Huang et al., 2020). The strategy relies on using thermodynamic sub-models for each device of the heat pump, explicitly considering their construction and operational parameters being as complex as required. Such simulation can capture transient behaviors of the cycle (Han et al., 2008) but, to simplify the simulation, a quasi steady-state approach has been commonly adopted to build scenarios or to assess equipment performance (Hirmiz et al., 2020).

Due to their user-friendly interfaces and powerful solvers, commercial software like TRNSYS®, MATLAB®, and Dymola® have been extensively used for simulating the operation of heat pumps (Palomba et al., 2019). Despite their

wide adoption, commercial platforms can be expensive, and sometimes integration with other systems can be limited, therefore instigating the development of open-source packages to simulate thermal systems. Open-source codes were employed in the study of heat pump parameters (Moreno et al., 2014; Shen et al., 2018; Cimmino and Wetter, 2017), or to build forecast scenarios for different systems integrating heat pumps (Carroll et al., 2020; Hilpert, 2020).

Among the available programming languages, Python is a high-level, general-purpose language that serves both linear and object-oriented programming (Lyden, 2020). Python is included in the Open Energy Modelling Initiative (Openmod, 2022), and some packages have been developed to model heat pumps. PyLESA, for instance, is a local energy system platform for Python that can be used for the simulation of heat pumps integrated to thermal and electric storage (Lyden et al., 2021). This open-source modeling package offers a Microsoft Excel interface that facilitates its use. Users may select among three approaches for COP calculation: (i) a Generic Regression Model, (ii) the Lorentz Model, and (iii) a Standard Test Regression Model. All of these are gray- or black-box models require manufacturer data or experimental results to build the regressions to predict the heat pump COP and capacity. TESPy—Thermal Engineering Systems in Python (Witte and Tuschy, 2020)—is another available collaborative package that embeds several thermal systems, is object-oriented, and includes heat pump components. Although the thermodynamic cycle is solved at each time-step, in the current available library the condenser and the evaporator are modeled as having only one phase in the refrigerant side. Moreover, the user interface is complex, and the learning curve may be steep. Other libraries are available in the official Python repository (Foundation, 2022), however, most of the options lack documentation.

In this work we present a quasi-steady heat pump model developed in Python 3 to simulate the operation of air-air and air-water heat pumps. The model includes construction parameters of the heat exchangers like tube length, fin ratio, and fin efficiency. Compressor rotation, displacement, and isentropic and volumetric efficiencies are considered to solve the thermodynamic cycle in each time step. Model validation and an application example are also provided in the paper. The proposed structure is flexible, allowing for simulating ASHP-TES with different components and operation conditions. The heat exchanger model is more detailed when compared with the existent packages, however, computational time is not compromised.

2. MODELING

Heat pumps operate a vapor compression cycle to transport energy from a relatively colder outside environment to the indoors through a vapor compression cycle. Although equipment presents several additional peripheral components, the basic cycle includes of a compressor, a condenser, an expansion device, and an evaporator. Aiming flexibility and future extrapolation the model was conceived in an object-oriented philosophy: each component (compressor, condenser, evaporator, and expansion vale) is an object, and they are combined in the greater object to represent the heat pump operation. The whole system is then composed of a heat pump, the residential thermal load, and a thermal storage device.

2.1 Vapor Compression Cycle

Figure 1a shows the schematic of a basic air-to-water heat pump integrated with sensible TES (a water tank). The heat pump is used to charge the TES, and water is recirculated from the TES tank to radiators to distribute heat in the home. All the equipment are modeled separately, hence, they can be replaced by regressions, gray-box, finite-volume (FV), or any other type of model.

Figure 1b shows the temperature-entropy diagram of the vapor compression cycle. The refrigerant mass flowrate in $\mathrm{kg\,s^{-1}}$ is calculated by

$$\dot{m}_r = \rho_1 V_{comp}\,(n/60)\,\eta_{vol}, \tag{1}$$

where V_{comp} is the displacement [m^3], n the compressor rotation speed [rpm], η_{vol} the volumetric efficiency. The energy balance on the condenser can be expressed by

$$\dot{Q}_c = \dot{m}_r(h_2 - h_3) \quad = \quad \dot{m}_r U_c A_c (T_{m_c} - T_{air_{indoor}}), \tag{2}$$

with h_2 and h_3 the specific enthalpies [kg/kJ] in the condenser inlet and outlet, respectively, U_c the overall heat transfer coefficient [$\mathrm{W\,m^{-2}\,K^{-1}}$], and A_c the condenser area [$\mathrm{m^2}$]. The average temperature of the refrigerant in the condenser is denoted by T_{m_c}. The expansion device is considered isenthalpic, therefore $h_4 = h_3$. In the evaporator, the energy

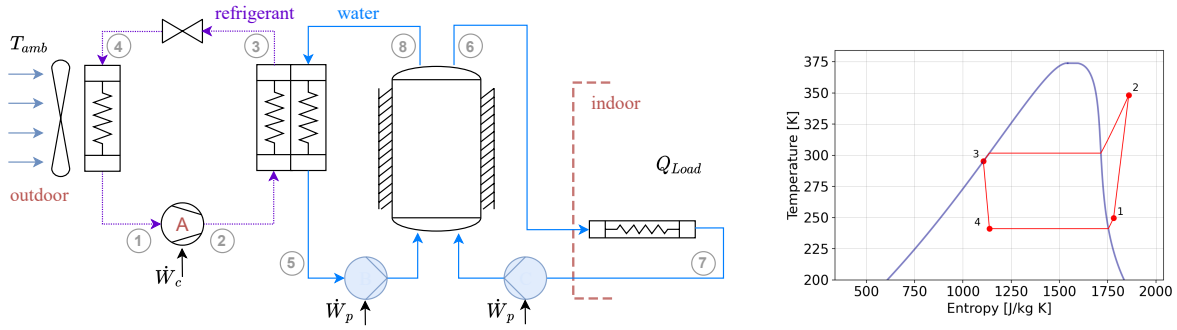

(a) System schematic **(b) T-S diagram**

Figure 1: Air-water air source heat pump integrated with sensible thermal energy storage.

balance is similar to the condenser so that

$$\dot{Q}_e = \dot{m}_r(h_1 - h_4) \quad = \quad \dot{m}_r U_e A_e (T_{m_e} - T_{air_{outdoor}}), \tag{3}$$

where U_e and A_e are the evaporator overall heat transfer coefficient and external surface area, respectively. T_{m_e} is the average temperature of the refrigerant in the evaporator. The heat exchange model for both condenser and evaporator is presented in the next section.

2.2 Heat Exchangers

A simple way of modeling heat exchangers is to assume they have a fixed effectiveness (Witte and Tuschy, 2020). Li et al. (2020), for instance, investigated the performance of a ASHP when charging a PCM storage tank, with a MATLAB® and TRNSYS® model with constant effectiveness in the condenser and evaporator. More detailed models can be employed to improve the accuracy of the results through finite volumes or finite elements, but they require a larger simulation time, which may limit their usage (Bonamente et al., 2016; Huang et al., 2020). In the current study for refrigerant-air heat exchangers (evaporator and condenser) we adopted the Kriging-assisted three-zone model proposed by Huang et al. (2020). This model can be up to 600 times faster than a finite volume approach, yet presents good accuracy (error $\leq$ 0.9 %). This model cannot be used for a refrigerant-water heat exchanger because the water temperature cannot be assumed as uniform. Therefore, for the refrigerant-water condenser we considered a constant effectiveness model.

The Kriging-assisted three-zone model considers the presence of three different regions in the heat exchanger with their respective phases, as presented in Figure 2. The refrigerant in the condenser is expected to have a super-heated (SH) refrigerant in the inlet, a 2-phase state in the middle region, and a sub-cooled (SC) state in the outlet. The length of each region will depend on the state of the refrigerant at the HX inlet and the external air temperature.

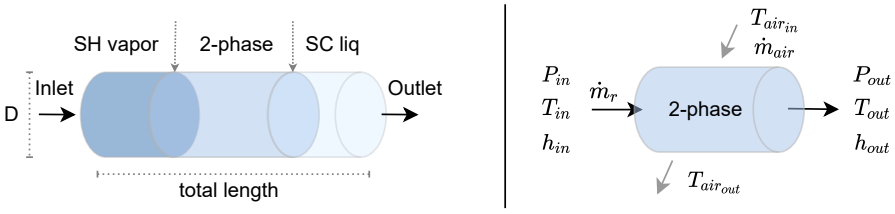

Figure 2: Kriging-assisted three-zone model (Huang et al., 2020) applied to the condenser.

The overall heat transfer coefficient, given in W m^{-2} K^{-1}, is calculated for each zone as (Li et al., 2020)

$$U_{zone} = \left(\frac{1}{h_z} + \frac{1}{h_{air}\eta_{fin}R_{fin}} \right)^{-1}, \tag{4}$$

Figure 3: Vapor compression solution scheme.

where h_z and h_{air} are the refrigerant-side and air-side heat transfer coefficients, respectively. η_{fin} stands for the fin's efficiency, and R_{fin} is the fin ratio. For the vapor and liquid phases, we assumed a representative heat transfer coefficient of $h_{vap} = h_{liq} = 600\,\mathrm{W\,m^{-2}\,K^{-1}}$, while for the 2-phase region it is $h_{2ph} = 3000\,\mathrm{W\,m^{-2}\,K^{-1}}$. h_{air} is assumed to be $100\,\mathrm{W\,m^{-2}\,K^{-1}}$. The adopted values are representative for the studied case, although they can vary depending on the fluids and the flow conditions. By performing an energy balance on each zone one can calculate the zone length (Eq. 5), outlet enthalpy (Eq. 6), or the outlet temperature (Eq. 7) (Huang et al., 2020).

$$L_{zone} = \frac{\dot{m}_r dh}{dT U_{zone} \pi D} \tag{5}$$

$$h_{zone} = h_{in} - U_{zone} A_{zone} \frac{dT}{\dot{m}_r} \tag{6}$$

$$T_{zone} = \frac{U_{zone} A_{zone} (T_{air_{in}} - 0.5 T_{in}) + \dot{m}_r * C_{p_r} * T_{in}}{(\dot{m}_r C_{p_r} + 0.5 U_{zone} A_{zone})} \tag{7}$$

The zone area is $A_{zone} = L_{zone} \pi D$ for a tube with diameter D and zone length L_{zone}, both in m. dh is the enthalpy variation along the zone, and dT is the difference between the zone mean temperature and $T_{air_{in}}$. The refrigerant-specific heat C_{p_r} ($\mathrm{J\,kg^{-1}\,K^{-1}}$) is evaluated at the zone inlet.

2.3 Thermal Load

The residential load factor method from standard 169-2021 (ANSI/ASHRAE, 2021) was used to simulate the heating load considering a detached single-family $120\,\mathrm{m^2}$ dwelling with the following features: walls ($A_w = 132\,\mathrm{m^2}$ and $U_w = 0.51\,\mathrm{W\,m^{-2}\,K^{-1}}$) and roof ($A_r = 120\,\mathrm{m^2}$ and $U_r = 0.18\,\mathrm{W\,m^{-2}\,K^{-1}}$). The thermal load is then calculated by

$$\dot{Q}_{load} = A_w U_w (T_{amb} - T_{sp}) + A_r U_r (T_{amb} - T_{sp}) \tag{8}$$

The indoor temperature setpoint T_{sp} is considered constant in the home.

2.4 Solution Scheme

Figure 3 displays the solution scheme, which was based on the enthalpy marching solution procedure (Winkler et al., 2008). After setting the system parameters, the pressures at points 1 and 2 are initially guessed. The energy balance is then applied for each equipment in the cycle, with a sub-cooling condition imposed to the condenser outlet (3) as well as a super-heating level imposed to the compressor inlet (1).

The SciPy optimization package (Virtanen et al., 2020) was employed to numerically solve the cycle, and the calculation is considered complete when the convergence criteria (residual $< 10^{-6}$) is satisfied. Usually, the COP and the system capacity are relevant results when assessing heat pumps (Bianco et al., 2017; Li et al., 2020). The former expresses the device efficiency when transporting thermal energy from the air outside to the indoor environment, and it is necessary to evaluate the compressor energy required to meet the heating loads.

3. MODEL ASSESSMENT

3.1 Validation with Experimental Data

The heat pump model was validated with experimental data reported by Shoukas et al. (2022), where a 35,000 Btu/h (10 263 W) commercial heat pump unit was evaluated in a controlled environment at the National Renewable Energy Laboratory (NREL). The model was fed with the parameters of the heat pump, so the predictions of the COP and the system capacity could be compared. Model and experimental results are presented in Figure 4 with the measurement

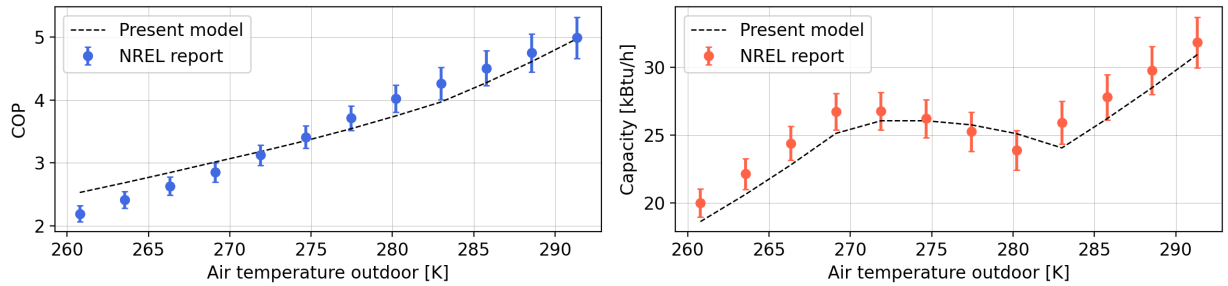

Figure 4: Validation with experimental data (Shoukas et al., 2022).

uncertainties. A maximum 10 % relative deviation was found for COP results, while the mean deviation for the entire range was 1.43 %. Regarding the system capacity, the model deviates 1.18 % from the experimental results on average, and the maximum deviation was 6.58 %. Model results show good agreement with the experimental data for the entire operation range, including the low temperature region, with the most significant deviations in the range of 275 K to 285 K.

3.2 Comparison with Heat Pump Simulator—Oak Ridge National Laboratory (ORNL)

We also compared the model with simulation results from the Heat Pump Design Model from Oak Ridge National Laboratory (2019) to increase our confidence on its accuracy. The parameters in Table 1 were provided to both models to compare COP and heating capacity, displayed in Figure 5. Over the simulated range of outdoor temperatures 264 K

Table 1: Parameters of the heat pump simulated in the ORNL model (Oak Ridge National Laboratory, 2019).

Parameter	Value	Unit
Compressor speed	3500	rpm
Isentropic efficiency	0.63	-
Volumetric efficiency	0.95	-
Displacement	5.37×10^{-5}	m^3
Refrigerant	R134a	-

Parameter	Value	Unit
Condenser air flow	0.47	$m^3\ s^{-1}$
Evaporator air flow	1.18	$m^3\ s^{-1}$
Condenser area	20.72	m^2
Evaporator area	41.87	m^2
Indoor temperature	294	K

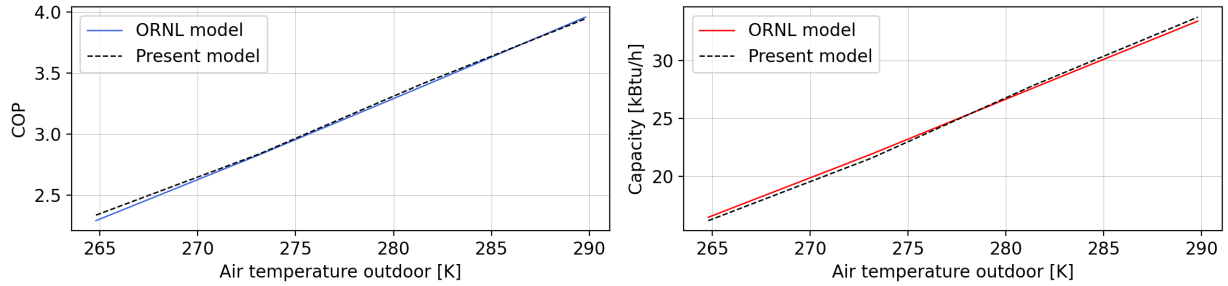

Figure 5: Comparison between ORNL heat pump simulator and the present model: COP and system capacity (Oak Ridge National Laboratory, 2019).

to 289 K, the maximum and average deviations for COP results were 1.98 % and 0.63 %, respectively. For the system capacity, the deviations were 1.79 % (max) and 0.4 % (average).

3.3 Sensitivity Analysis

A sensitivity analysis was performed with the independent input variables $T_{air,outdoor}$ varying from 250 K to 290 K and the condenser inlet temperature T_8 in the range of 295 K to 330 K. A Sobol's sampling with n^{12} resulted in 24,576 simulated points (Saltelli et al., 2008). Polynomial regressions were built from 70 % of the data set, while the remaining

30 % was used to verify the regression quality, which presented a 0.019 root mean square error. Results indicate that the COP has a similar correlation to $T_{air,outdoor}$ and T_8 (approx. 0.51), as shown in Figure 6a. Heat capacity is strongly correlated to $T_{air,outdoor}$ and weakly correlated to T_8, Figure 6b.

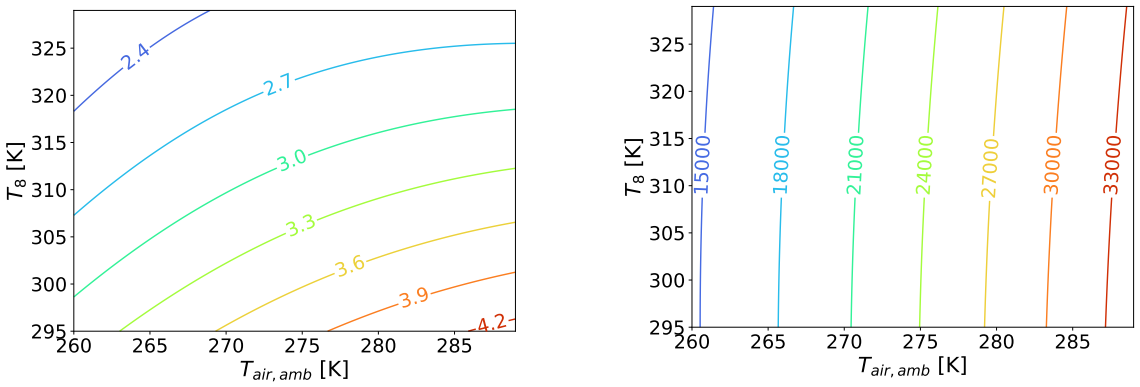

(a) COP

(b) Heating capacity [BTU/h]

Figure 6: Contour plots for COP and heating capacity as a function of the ambient air temperature $T_{air,outdoor}$, and the condenser temperature T_8.

4. ASHP-TES INTEGRATION

To illustrate the model capability of representing the integration between a heat pump and a thermal storage device, an application example is presented. Table 2 shows the parameters adopted for the system (Figure 1). An artificial sinusoidal temperature profile varying from 265 K to 285 K was imposed to T_{amb} to assess the model response. Moreover, an initial state of charge (SOC) = 15 % was considered for the TES.

Table 2: System parameters adopted in the example.

Device	Parameter	Value
Compressor	n	3600
	$Disp$	5.37×10^{-5}
	η_{iso}	0.63
	η_{vol}	0.95
Condenser	Effectiveness	0.7
Water tank	Area	6.28 m^2
	Volume	1.17 m^3
	Overall heat transfer coeff. U	1 $W\,m^{-2}\,K^{-1}$
Pump B	Mass flow rate	0.1 $kg\,s^{-1}$

The example considered the system operating under four different modes, as observed in Table 3. If $T_{outdoor} > 270$ and $Q_{load} > 0$ mode 1 is adopted. Mode 2 is adopted if the ambient temperature is lower than 270 K and the SOC of TES is > 10 %. Whenever $Q_{load} = 0$, no heat transfer to the indoors takes place (mode 3). In this situation if the SOC is less than 95 % the heat pump is used to charge the TES. Mode 4 is assumed when $\dot{Q}_{load} = 0$ and SOC > 95 %. The logic of Table 3 is a basic approach to operate an ASHP-TES system. More elaborated strategies can be explored and depends on the system goals. For example, if the electricity rate differs depending on the hour of the day, one may want to shift the heating load by using the system of Figure 3. Another example is the integration with renewables like solar and wind. In this case the system can introduce flexibility by supplying the heating loads in times when renewables are not available.

Figure 7a displays the state of charge of the TES, the operation mode, and the outdoor temperature over 24 h of oper-

Table 3: ASHP-TES operation logic adopted for this example.

Mode	Heat pump	Thermal storage	Temp. outdoor [K]	Thermal load [W]
1	ON	Charging/Discharging	> 270	> 0
2	OFF	Discharging	< 270	> 0
3	ON	Charging	> 270	= 0
4	OFF	OFF	> 270	= 0

ation. Due to the imposed rules, the system only assumed operation modes 3, 1, and 2 while mode 4 was never in use. During the first 10 hours the system is charging the TES and supplying $\dot{Q}_{load}$, modes 3 and 1. In the following hours

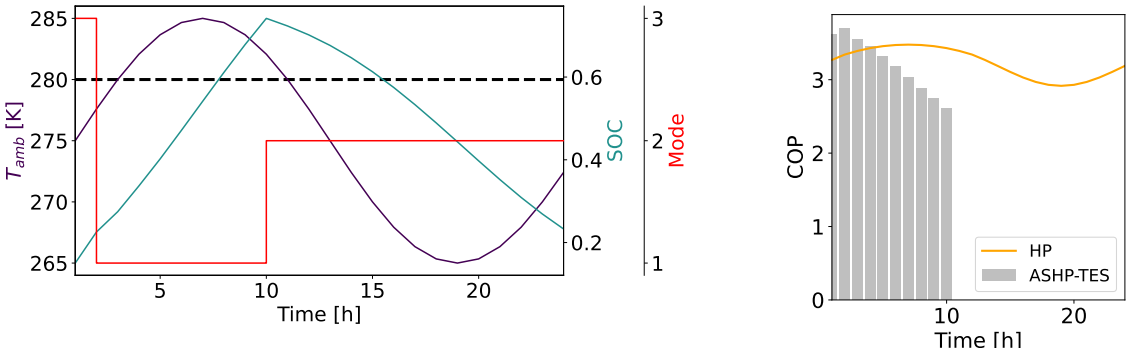

(a) SOC and MODE **(b)** COP

Figure 7: System operation mode and COP results over time.

mode 2 is activated and TES is discharged from SOC = 80 % to 25 %. Figure 7b displays the system COP for the same time range. It is interesting to note that although T_{amb} is increasing in time 0 h to 10 h the system COP is decreasing. This occurs because T_8 is also increasing with the TES SOC. Additionally, from time 10 h to 24 h the system COP is zero because the TES is in discharge mode and the heat pump is off.

Figure 8 shows the temperature of the relevant points of the vapor compression cycle and the water circuit for the same time window. T_2 is the temperature of the refrigerant entering the condenser, hence it is only presented when the heat pump is on. T_5, the water leaving the condenser, follows T_2 trend, while T_6 and T_8 represent the water temperature in the tank. Regarding computational time, the model took 8 s to complete the 24 h simulation in a windows-based computer (CPU Intel® Core i7-9750H CPU @2.6 GHz, 16 Gb RAM DDR4), which indicates computational time of 600 s for annual simulations. Several arrangements and operation strategies may be envisioned for ASHP-TES systems. It may be used for peak-shaving and load shifting, specially observing different electricity rates. The use of TES may also prevent the heat pump from operating under extremely low temperatures, where the heat pump performance is lower.

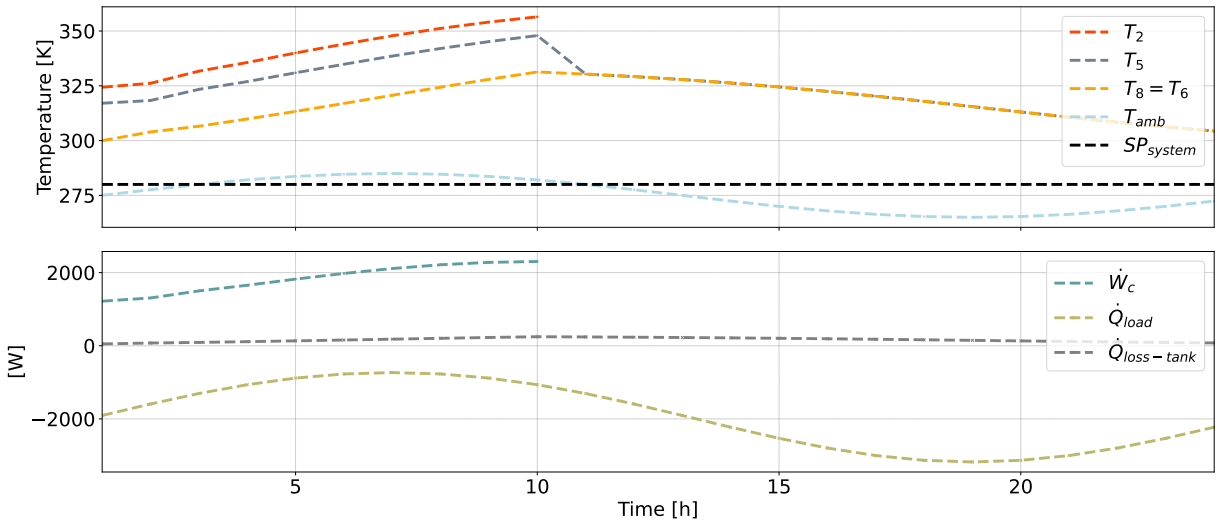

Figure 8: Temperatures in relevant points of the system and the heat exchange levels.

5. CONCLUSIONS

In this study we developed a Python package to simulate air source heat pumps integrated with thermal energy storage. The model solves the thermodynamic states of each component by following an enthalpy marching solver solution procedure. The framework was built in a modular philosophy to facilitate further investigation with different equipment and sub models. A Kriging-assisted three-zone model was adopted to solve the refrigerant-air condenser and evaporator. For the refrigerant-water condenser, the effectiveness was set constant. Validation with experimental data obtained from a real heat pump is provided, with maximum and average deviations of 10 % and 1.43 % for COP results and 6.58 % and 1.18 % for the system capacity. An example of how the model can be used to assess AHSP-TES integration was presented, with the system operating over 24 h. Results demonstrate the model capability in representing the system operation and allows for simulations in different time-steps. Given the low computational effort further analyses in a annual base can now be developed for different locations in a reasonable time (approx. 600 s).

NOMENCLATURE

Latin Symbols

A	Area	(m^2)
C_p	Specific heat at constant pressure	($J\,kg^{-1}\,K^{-1}$)
h	Specific enthalpy	($J\,kg^{-1}$)
h	Convective heat transfer coefficient	($W\,m^{-2}\,K^{-1}$)
ID	Inner diameter	(m)
L	Length	(m)
$\dot{m}$	Mass flow rate	($kg\,s^{-1}$)
n	Angular speed	(rpm)
$\dot{Q}$	Heat transfer rate	(W)
R_{fin}	Fin thermal resistance	($W\,m^{-2}\,K^{-1}$)
T	Temperature	(K)
U	Overall heat transfer coefficient	($W\,m^{-2}\,K^{-1}$)
V	Displacement	(m^3)

Greek Symbols

η	Efficiency	(-)
ρ	Specific mass	($kg\,m^{-3}$)

Subscripts

amb	Ambient
comp	Compressor
c	Condenser
e	Evaporator
m	Average
p	Pressure
r	Refrigerant
vol	Volumetric
z	Zone

REFERENCES

ANSI/ASHRAE (2021). ANSI/ASHRAE Standard 169-2021 - Climatic Data for Building Design Standards. Technical report, ANSI/ASHRAE, Peachtree Corners.

Bianco, V., Scarpa, F., and Tagliafico, L. A. (2017). Estimation of primary energy savings by using heat pumps for heating purposes in the residential sector. *Applied Thermal Engineering*, 114:938–947.

Bonamente, E., Aquino, A., and Cotana, F. (2016). A PCM Thermal Storage for Ground-source Heat Pumps: Simulating the System Performance via CFD Approach. *Energy Procedia*, 101(September):1079–1086.

Carroll, P., Chesser, M., and Lyons, P. (2020). Air Source Heat Pumps field studies: A systematic literature review. *Renewable and Sustainable Energy Reviews*, 134.

Cimmino, M. and Wetter, M. (2017). Modelling of Heat Pumps with Calibrated Parameters Based on Manufacturer Data. *Proceedings of the 12th International Modelica Conference, Prague, Czech Republic, May 15-17, 2017*, 132(2002):219–226.

Dincer, I., Rosen, M. A., and Ahmadi, P. (2017). *Optimization of Energy Systems*. John Wiley and Sons Ltd, 1 edition.

Foundation, P. S. (2022). Python Repository.

Han, Z., Zheng, M., Kong, F., Wang, F., Li, Z., and Bai, T. (2008). Numerical simulation of solar assisted ground-source heat pump heating system with latent heat energy storage in severely cold area. *Applied Thermal Engineering*, 28(11-12):1427–1436.

Hilpert, S. (2020). Effects of decentral heat pump operation on electricity storage requirements in Germany. *Energies*, 13(11).

Hirmiz, R., Teamah, H. M., Lightstone, M. F., and Cotton, J. S. (2020). Analytical and numerical sizing of phase change material thickness for rectangular encapsulations in hybrid thermal storage tanks for residential heat pump systems. *Applied Thermal Engineering*, 170.

Huang, R., Ling, J., and Aute, V. (2020). Comparison of approximation-assisted heat exchanger models for steady-state simulation of vapor compression system. *Applied Thermal Engineering*, 166(November 2019):114691.

Le, K. X., Huang, M. J., Shah, N., Wilson, C., Artain, P. M., Byrne, R., and Hewitt, N. J. (2019). High temperature air source heat pump coupled with thermal energy storage: Comparative performances and retrofit analysis. *Energy Procedia*, 158:3878–3885.

Li, Y., Zhang, N., and Ding, Z. (2020). Investigation on the energy performance of using air-source heat pump to charge PCM storage tank. *Journal of Energy Storage*, 28.

Lyden, A. (2020). *Modelling and Design of Local Energy Systems Incorporating Heat Pumps, Thermal Storage, Future Tariffs, and Model Predictive Control*. PhD thesis, University of Strathclyde.

Lyden, A., Flett, G., and Tuohy, P. G. (2021). PyLESA: A Python modelling tool for planning-level Local, integrated, and smart Energy Systems Analysis. *SoftwareX*, 14:100699.

Moreno, P., Sole, C., Castell, A., and Cabeza, L. F. (2014). The use of phase change materials in domestic heat pump and air-conditioning systems for short term storage: A review. *Renewable and Sustainable Energy Reviews*, 39:1–13.

Oak Ridge National Laboratory (2019). DOE/ORNL Heat Pump Design Model.

Openmod (2022). Open Energy Modelling (openmod) Initiative.

Palomba, V., Varvagiannis, E., Karellas, S., and Frazzica, A. (2019). Hybrid adsorption-compression systems for air conditioning in efficient buildings: Design through validated dynamic models. *Energies*, 12(6).

Saltelli, A., Ratto, M., Andres, T., Campolongo, F., Cariboni, J., Gatelli, D., Saisana, M., and Tarantola, S. (2008). *Global Sensitivity Analysis. The Primer*. John Wiley & Sons Inc, West Sussex, England, 1 edition.

Shen, B., Nawaz, K., Baxter, V., and Elatar, A. (2018). Development and validation of quasi-steady-state heat pump water heater model having stratified water tank and wrapped-tank condenser. *International Journal of Refrigeration*, 87:78–90.

Shoukas, G., Bonnema, E., Paranjothi, G., Faramarzi, R., Klun, L., Shoukas, G., Bonnema, E., Paranjothi, G., Faramarzi, R., and Klun, L. (2022). Performance Assessment of High Efficiency Variable Speed Air-Source Heat Pump in Cold Climate Applications. Technical Report February, National Reneable Energy Laboratory (NREL), Golden, CO.

Virtanen, P., Gommers, R., Oliphant, T. E., Haberland, M., Reddy, T., Cournapeau, D., Burovski, E., Peterson, P., Weckesser, W., Bright, J., van der Walt, S. J., Brett, M., Wilson, J., Millman, K. J., Mayorov, N., Nelson, A. R. J., Jones, E., Kern, R., Larson, E., Carey, C. J., Polat, I., Feng, Y., Moore, E. W., VanderPlas, J., Laxalde, D., Perktold, J., Cimrman, R., Henriksen, I., Quintero, E. A., Harris, C. R., Archibald, A. M., Ribeiro, A. H., Pedregosa, F., van Mulbregt, P., and SciPy 1.0 Contributors (2020). SciPy 1.0: Fundamental Algorithms for Scientific Computing in Python. *Nature Methods*, 17:261–272.

Winkler, J., Aute, V., and Radermacher, R. (2008). Comprehensive investigation of numerical methods in simulating a steady-state vapor compression system. *International Journal of Refrigeration*, 31(5):930–942.

Witte, F. and Tuschy, I. (2020). TESPy: Thermal Engineering Systems in Python. *Journal of Open Source Software*, 5(49):2178.

ACKNOWLEDGEMENT

This study was financed in part by the Coordenação de Aperfeiçoamento de Pessoal de Nível Superior - Brasil (CAPES) - Finance Code 001. Conrado Ermel acknowledges Conselho Nacional de Desenvolvimento Científico e Tecnológico (CNPq) for his Ph.D. grant. Paulo S. Schneider acknowledges CNPq for his research grant (PQ305357/2013-1). This work was authored in part by the National Renewable Energy Laboratory, operated by Alliance for Sustainable Energy, LLC, for the U.S. Department of Energy (DOE) under Contract No. DE-AC36-08GO28308. Funding provided by the U.S. Department of Energy Office of Energy Efficiency and Renewable Energy Building Technologies Office. The views expressed in the article do not necessarily represent the views of the DOE or the U.S. Government. The U.S. Government retains and the publisher, by accepting the article for publication, acknowledges that the U.S. Government retains a nonexclusive, paid-up, irrevocable, worldwide license to publish or reproduce the published form of this work, or allow others to do so, for U.S. Government purposes.